

Influence of magnetism on superconductivity in epitaxial Fe/Nb bilayer systems

Th. Mühge, K. Theis-Bröhl, K. Westerholt, and H. Zabel

Institut für Experimentalphysik/Festkörperphysik, Ruhr-Universität Bochum, D-44780 Bochum, Germany

N. N. Garif'yanov, Yu. V. Goryunov, and I. A. Garifullin

Kazan Physicotechnical Institute of Russian Academy of Sciences, 420029 Kazan, Russian Federation

G. G. Khaliullin*

Max-Planck Institut für Physik komplexer Systeme, D-01187 Dresden, Germany

(Received 27 May 1997; revised manuscript received 22 August 1997)

We studied the superconductivity of molecular-beam-epitaxy-grown epitaxial Nb(110) thin films covered by Fe(110) monocrystalline layers with thicknesses d_{Fe} between 4 and 30 Å. We find a nonmonotonous dependence of the superconducting transition temperature T_c on d_{Fe} , however, without a maximum in $T_c(d_{\text{Fe}})$ as observed earlier in Nb/Fe layers prepared by sputtering techniques. We argue that the change in the $T_c(d_{\text{Fe}})$ curve is caused by a smaller thickness of the nonmagnetic Fe-rich interlayer at the Nb/Fe interface and can be explained within the same model developed previously for the explanation of the maximum in $T_c(d_{\text{Fe}})$ in sputtered Nb/Fe layers. [S0163-1829(98)04209-X]

The study of superconductivity in multilayer systems combined of ferromagnetic (FM) and superconducting (SC) layers is a topic of great current interest (see, e.g., Refs. 1–3 and references therein). The renewed interest in this classical proximity effect at a FM/SC interface⁴ partly originates from the observation of a maximum in the SC transition temperature T_c in several systems,^{1,2} when plotting T_c versus the thickness of the FM-layer d_F . This has given rise to the speculation that the FM/SC multilayer systems might represent the first experimental example of a π -type Josephson coupling between successive SC layers, which has been predicted theoretically.⁵

In our recent study on Fe/Nb/Fe-trilayer systems,^{6,7} for which a π -type coupling can be excluded for geometrical reasons, we found, however, a similar $T_c(d_{\text{Fe}})$ curve with a clearly resolvable maximum at $d_{\text{Fe}} \approx 12$ Å. We have developed a new model for the interpretation of the peculiar $T_c(d_{\text{Fe}})$ dependence in Fe/Nb, taking the presence of a nonmagnetic (magnetically “dead”) Fe-rich interlayer at the Nb/Fe interface into consideration. This interlayer acts in a twofold manner. On the one hand it reduces T_c due to the introduction of a strongly repulsive interaction for the Cooper pairs. On the other hand, it screens the SC layer from the strongly pair-breaking exchange field of the FM layer. As explained in detail in Ref. 7 with an appropriate thickness of the nonmagnetic interlayer the onset of ferromagnetism in the Fe layer can cause an enhancement of T_c first, instead of a rapid suppression of T_c , which would be expected considering proximity effects between the FM layer and the SC layer alone.

Since the interlayer at the Fe/Nb interface plays an essential role in our model, the aim of the present paper is a comparative study of $T_c(d_{\text{Fe}})$ for heterostructures prepared in single crystalline form by the molecular beam epitaxy (MBE) technique. The optimized growth of Fe on Nb by state of the art MBE techniques is known to provide the

highest quality interface with less alloying than in the case of sputtered systems. This might lead to a change of the $T_c(d_{\text{Fe}})$ dependence.

The Nb/Fe bilayers were prepared by a conventional 3-in. RIBER EVA 32 metal molecular beam epitaxy system (for details about this equipment see, e.g., Ref. 8). The base pressure in the sample chamber is 5×10^{-9} Pa and the working pressure 2×10^{-8} Pa. Nb was evaporated by electron beam evaporation from a 14-cm³ crucible. An evaporation rate of 0.5 Å/s was found to be optimal for the growth of high quality single crystal Nb(110) films with SC transition temperature $T_c = 8.5$ K. Fe was deposited from an effusion cell providing a flux of high stability. A rate of 0.1 Å/s was used and the final thickness was determined by the evaporation time. The placement of the effusion cells is inclined at a certain angle to the 3-in. sample holder. This gave us the opportunity for the preparation of an Fe wedge on top of the Nb layers. As substrate material a single crystal Al₂O₃ (11 $\bar{2}$ 0) was used, which was outgassed and finally annealed at 1000 °C for more than 1 h before starting the evaporation process. The substrate temperature during the evaporation of the first Nb layer was 900 °C. Subsequently the layer was annealed at 950 °C for 15 min. The following Fe wedge type layer was evaporated at 100 °C. Finally the Fe wedge was covered by a thin Nb and Pd film of 30 Å thickness in order to prevent Fe from oxidation. The quality of each layer was controlled by *in situ* reflection high-energy electron diffraction characterization. We have prepared three samples with wedge-shaped Fe layers: m855 with $d_{\text{Nb}} = 220$ Å and with $d_{\text{Fe}} = 10 \cdot 26$ Å; m856 with $d_{\text{Nb}} = 250$ Å and with $d_{\text{Fe}} = 7 \cdot 23$ Å; m879 with $d_{\text{Nb}} = 225$ Å and with $d_{\text{Fe}} = 4 \cdot 9$ Å. The width of each sample was 50 mm. For the magnetization, resistivity, and ac-susceptibility measurements the samples were cut into stripes with a width of 3 mm.

X-ray reflectivity measurements were performed *ex situ* at three positions of each sample, using an additional vertical slit of 0.2 mm in order to exclude effects from the Fe gradi-

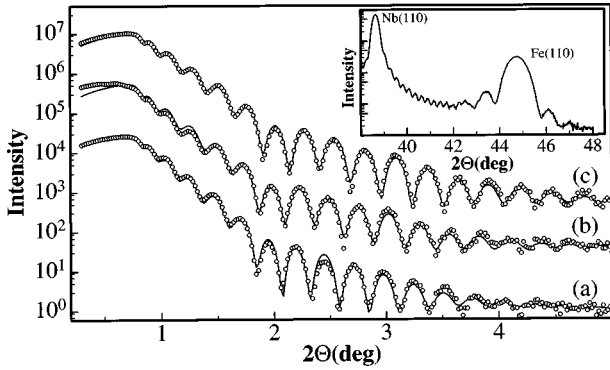


FIG. 1. X-ray reflectivity scans taken on three films cut from the m855 sample. The solid line is a fit by the Parratt formalism (Ref. 9). The Fe thickness as determined from the fit was (a) 10 Å, (b) 15 Å, and (c) 23 Å. The inset shows the (110) Bragg reflections with well resolved Laue oscillations.

ent on the interpretation of the spectra. In Fig. 1 three typical reflectivity measurements are presented for films cut from the sample m855 with $d_{\text{Fe}} = 10, 15,$ and 23 Å, respectively, showing well resolved thin film thickness oscillations (Kiessig fringes). The broadening of the total reflectivity edge is due to the top Pd layer with a rather high electron density and a correspondingly high critical angle. Fits with the Parratt formalism⁹ shown as solid lines in Fig. 1 give interface roughnesses of less than 5 Å, indicating the high structural quality of our samples. The film thicknesses obtained from these fits were used for the final calibration of d_{Fe} .

The inset of Fig. 1 shows a typical Bragg scan of a sample with $d_{\text{Nb}} = 350$ Å and $d_{\text{Fe}} = 100$ Å. The presence of Laue oscillations from the Nb as well as the Fe layers is an indication of the structural coherence of the films. All samples show (110) growth of Nb and Fe with a structural coherence length comprising the total film thickness. In-plane x-ray Bragg reflection measurements by grazing incidence diffraction show that Fe and Nb grow within a single domain with the Fe[001] axis parallel to the Nb[001] axis.

The magnetic state of the Fe layers was studied by a superconducting quantum interference device magnetometer at a temperature of 10 K with the surface of the samples parallel to the magnetic field. In Fig. 2 the saturation magnetiza-

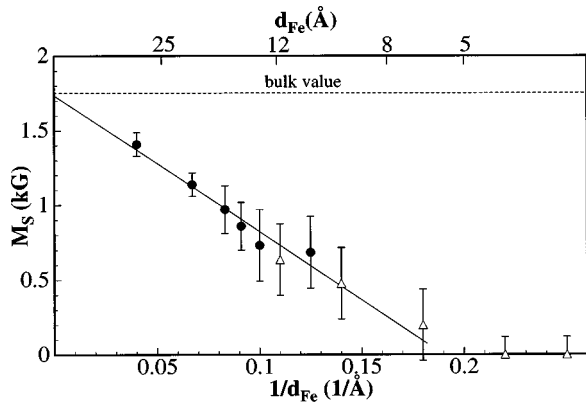


FIG. 2. Saturation magnetization versus reciprocal thickness of the Fe-layer $1/d_{\text{Fe}}$ for a series of films cut from the m855 (closed circles) and m879 (opened triangles) samples. The solid line is a linear fit.

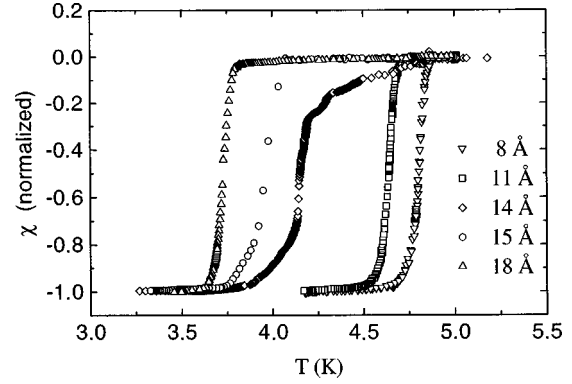


FIG. 3. Transition curves as obtained by ac susceptibility for five samples with different d_{Fe} cut from the m856 sample.

tion as a function of $1/d_{\text{Fe}}$ is presented for a series of films cut from m855 and m879 samples. The saturation magnetization values are determined using the Fe thickness d_{Fe} as obtained by the x-ray reflectivity measurements.

For the residual resistivity ratio $RRR = R_{300\text{ K}}/R_{10\text{ K}}$ we obtained a factor of about 10–15 for all of our samples. Taking the phonon resistivity of bulk Nb as $\rho_{\text{ph}} = 14.5$ $\mu\Omega$ cm, we estimate a residual resistivity of less than 1.6 $\mu\Omega$ cm for our samples. Using the experimental values for the density of states at ϵ_F and the Fermi velocity for Nb, we obtain $\langle \rho l \rangle = 3.75 \times 10^{-6}$ $\mu\Omega$ cm²,¹⁰ corresponding to a mean free path of 250 Å. According to Ref. 5 the value of the SC coherence length can be estimated by

$$\xi_S = \sqrt{\frac{\xi_{\text{BCS}} l}{3.4}}$$

where ξ_{BCS} is the BCS coherence length of pure Nb. We then obtain $\xi_S = 180$ Å for our thin films, which is three times larger than the ξ_S estimated for our sputtered films.⁷

The SC transition temperature T_c was measured by ac susceptibility. Typical transitions for one series of samples are presented in Fig. 3. Except for the sample with $d_{\text{Fe}} = 14$ Å, all transitions are very sharp. The origin for the slightly broader transition of the sample with $d_{\text{Fe}} = 14$ Å can be understood by taking into account the shape of the $T_c(d_{\text{Fe}})$ curve (see Fig. 4), with the strong thickness dependence around $d_{\text{Fe}} = 14$ Å. Hence a small gradient of d_{Fe} caused by the wedge shape of the Fe layer can lead to a definite broadening of the SC transition.

The SC transition temperature T_c , defined as the midpoint of the ac-susceptibility transition, is plotted in Fig. 4 for three series of samples with variable d_{Fe} and fixed d_{Nb} . As mentioned above, T_c for a pure SC Nb film is about 8.5 K. Thus there is a strong initial T_c suppression at lower d_{Fe} followed by a flat $T_c(d_{\text{Fe}})$ curve for $5 \text{ Å} \leq d_{\text{Fe}} \leq 13 \text{ Å}$ and final dropping to a constant lower T_c value between $13 \text{ Å} \leq d_{\text{Fe}} \leq 16 \text{ Å}$.

Thus in the present Fe/Nb bilayers T_c depends nonmonotonously on d_{Fe} , similar to our previously studied Fe/Nb/Fe trilayers,^{6,7} however, here without a maximum in $T_c(d_{\text{Fe}})$. It is necessary to note that a strong resemblance exists between our data and the data reported on the Nb/Gd system,^{2,3} when comparing sputtered and MBE samples. In both cases the sputtered samples show an increase in T_c

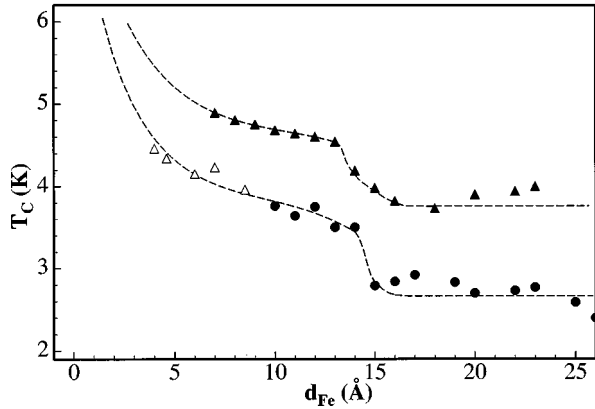


FIG. 4. Superconducting transition temperature T_c versus d_{Fe} for three series of samples (closed triangles: m856; closed circles: m855; opened triangles: m879). The broken lines are guides for the eye.

when the magnetic layer becomes FM, while the MBE samples show a shoulderlike feature with a downward jump around $13 \cdots 20 \text{ \AA}$. We believe that for both systems the change of the T_c dependence on the “magnetic” layer thickness is due to a smaller value of the non FM interlayer at the interface in the MBE samples compared to the sputtered samples.

The linear dependence of M_S on $1/d_{\text{Fe}}$ (Fig. 2) is caused by the presence of a nonmagnetic Fe/Nb at the interface.^{6,7} A linear fit gives a thickness of the nonmagnetic layer of $d_{\text{NM}} \approx 5 \text{ \AA}$. This is smaller than d_{NM} for Fe/Nb/Fe trilayers prepared by rf sputtering techniques,⁷ where the magnetically “dead” layer thickness was larger than 7 \AA . We have assumed⁷ that the magnetically “dead” layer arises due to an intermixing of Nb and Fe at the interface. Therefore the difference in the nonmagnetic layer thickness may be due to the smaller particle energies during thermal evaporation as compared to sputtering. It is well known that Fe atoms diluted in Nb lose their magnetic moment. This has been experimentally established¹¹ and theoretically explained.¹²

Let us discuss the observed $T_c(d_{\text{Fe}})$ dependence. From our magnetization data we concluded that for $d_{\text{Fe}} < d_{\text{NM}}$ ferromagnetism is absent. As explained in detail in Ref. 7, the effective electron-electron interaction in this Fe-rich nonmagnetic interlayer is strongly repulsive and stems from the coupling of the conduction electrons to the local paramagnon fluctuations. This repulsive interaction suppresses T_c by the proximity effect thus giving rise to the initial T_c suppression in Fig. 4. A special situation is given when a FM Fe layer occurs first for $d_{\text{Fe}} > d_{\text{NM}}$, since then there are two competing effects:

(a) The Zeeman splitting of the virtual Fe-derived d state in the nonmagnetic layer weakens the repulsive interaction and this enhances T_c .⁷

(b) The exchange field of the FM layer is strongly pair breaking and reduces T_c . If one assumes ideally transparent interfaces and neglects any influence of spin-orbit interaction, one can easily estimate the expected T_c suppression. The exchange splitting of the conduction band in Fe I_{Fe} is about 1 eV . In the Cooper limit the effective exchange field acting on the Cooper pairs in the Fe layer is given by

$$I_{\text{eff}} = I_{\text{Fe}}(d_{\text{Fe}}/d_{\text{Nb}}). \quad (1)$$

Considering the Clogston limit, a field of $H = \sqrt{2}\Delta/g\mu_B$ will completely quench superconductivity. With the gap parameter Δ for Nb and the exchange field $H = I_{\text{eff}}/\mu_B$ a complete quenching of superconductivity is expected for $d_{\text{Fe}} \approx 0.5 \text{ \AA}$. This corresponds to less than one monolayer.

In the sputtered Fe/Nb/Fe trilayers the FM layer is well screened by the nonmagnetic interlayer and effect (a) dominates. This give rise to the T_c maximum just at the onset of ferromagnetism.

In the MBE-grown samples, the nonmagnetic interlayer is thinner, thus the FM layer is less well screened and has a stronger direct negative influence on T_c . Both effects (a) and (b) just compensate and give rise to the first plateau in $T_c(d_{\text{Fe}})$ in Fig. 4. At larger d_{Fe} the negative direct effect of the exchange field dominates in any case and a downward jump in $T_c(d_{\text{Fe}})$ with a large slope is expected. T_c approaches a second plateau at an FM layer thickness $d = d_{\text{Fe}} - d_{\text{NM}}$ comparable to the penetration depth of Cooper pairs into the Fe layer $\xi_M \sim 12 \text{ \AA}$.¹³ It is necessary to note that the absence of any anomaly in the magnetization at the Fe thickness range between 5 and 25 \AA (Fig. 2) indicates that the jump in the $T_c(d_{\text{Fe}})$ curve at $13 \cdots 16 \text{ \AA}$ is caused by the exchange field only.

In summary, we have studied the influence of magnetism on the superconductivity in high quality epitaxial Fe/Nb bilayers. We obtained a nonmonotonous $T_c(d_{\text{Fe}})$ curve, however, without the maximum observed in our sputtered samples. We explained this finding in the model developed previously for sputtered Fe/Nb/Fe trilayers.⁷ This model was based on a combined action of the FM Fe layer and the nonmagnetic Fe/Nb interface on the superconductivity. We concluded that the actual shape of the $T_c(d_{\text{Fe}})$ curve in Fe/Nb multilayers is mainly determined by the thickness of the nonmagnetic interface. Therefore FM/SC proximity systems offer an additional tool for the study of interface regions and its complex interplay with the physical properties in multilayer system.

We would like to thank J. Podschwadeck and C. Leschke for technical support. This work was supported by the Deutsche Forschungsgemeinschaft (Grant No. DFG-ZA161/6-2) and by the Russian Fund for Fundamental Research (Project No. 96-02-16332a), which are gratefully acknowledged. One of us (I.A.G.) acknowledges NATO support under the collaborative research Grant No. HTECH .CRG961371.

*Permanent address: Kazan Physicotechnical Institute of Russian Academy of Sciences, 420029 Kazan, Russian Federation.

¹H. K. Wong, B. Y. Jin, H. Q. Yang, J. B. Ketterson, and J. E. Hillard, *J. Low Temp. Phys.* **63**, 307 (1986).

²J. S. Jiang, D. Davidović, Daniel H. Reich, and C. L. Chien, *Phys. Rev. Lett.* **74**, 314 (1995).

³C. Strunk, C. Sürgers, U. Paschen, and H. v. Löhneysen, *Phys. Rev. B* **49**, 4053 (1994).

- ⁴N. R. Werthamer, Phys. Rev. **132**, 2440 (1963).
- ⁵Z. Radović, M. Ledvij, L. Dobrosavljević-Grujić, A. I. Buzdin, and J. R. Clem, Phys. Rev. B **44**, 759 (1991), and references therein.
- ⁶Th. Mühge, N. N. Garif'yanov, Yu. V. Goryunov, G. G. Khaliullin, L. R. Tagirov, K. Westerholt, I. A. Garifullin, and H. Zabel, Phys. Rev. Lett. **77**, 1857 (1996).
- ⁷Th. Mühge, K. Westerholt, H. Zabel, N. N. Garif'yanov, Yu. V. Goryunov, I. A. Garifullin, and G. G. Khaliullin, Phys. Rev. B **55**, 8945 (1997).
- ⁸K. Theis-Bröhl, R. Scheidt, Th. Zeidler, F. Schreiber, H. Zabel, Th. Mathieu, C. Mathieu, and B. Hillebrands, Phys. Rev. B **53**, 11 613 (1996).
- ⁹L. G. Parratt, Phys. Rev. **95**, 354 (1954).
- ¹⁰H. Weber, E. Seidl, C. Laa, E. Schachinger, M. Prohammer, A. Junod, and D. Eckert, Phys. Rev. B **44**, 7585 (1991).
- ¹¹B. T. Matthias, W. Peter, H. J. Williams, A. M. Clogston, E. Corenzwit, and R. C. Sherwood, Phys. Rev. Lett. **5**, 542 (1960).
- ¹²P. Lang, B. Dittler, R. Zeller, and P. H. Dederichs, J. Phys.: Condens. Matter **4**, 911 (1992).
- ¹³G. Verbanck, C. D. Potter, R. Schad, P. Belien, V. V. Moschalkov, and Y. Bruynseraede, Physica C **235-240**, 3295 (1994).